

Journal of Materials Chemistry C

Accepted Manuscript



This article can be cited before page numbers have been issued, to do this please use: J. Quinn, F. Haider, H. D. Patel, D. A. Khan, Z. Y. Wang and Y. Li, *J. Mater. Chem. C*, 2017, DOI: 10.1039/C7TC03023A.



This is an Accepted Manuscript, which has been through the Royal Society of Chemistry peer review process and has been accepted for publication.

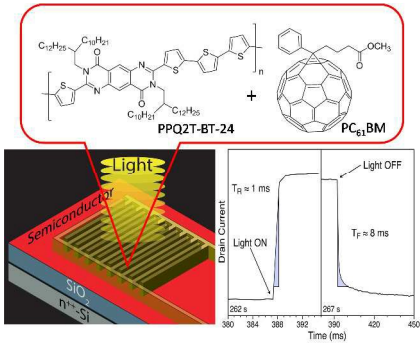
Accepted Manuscripts are published online shortly after acceptance, before technical editing, formatting and proof reading. Using this free service, authors can make their results available to the community, in citable form, before we publish the edited article. We will replace this Accepted Manuscript with the edited and formatted Advance Article as soon as it is available.

You can find more information about Accepted Manuscripts in the [author guidelines](#).

Please note that technical editing may introduce minor changes to the text and/or graphics, which may alter content. The journal's standard [Terms & Conditions](#) and the ethical guidelines, outlined in our [author and reviewer resource centre](#), still apply. In no event shall the Royal Society of Chemistry be held responsible for any errors or omissions in this Accepted Manuscript or any consequences arising from the use of any information it contains.

Graphical abstract

A pyrimido[4,5-g]quinazoline-4,9-dione (PQ) based polymer, PPQ2T-BT-24, is used as a photosensitive and charge transport semiconductor for ultrafast organic phototransistors (OPTs).





Journal Name

COMMUNICATION

Ultrafast photoresponse organic phototransistors based on pyrimido[4,5-*g*]quinazoline-4,9-dione polymer

Received 00th January 20xx,
Accepted 00th January 20xxJesse T. E. Quinn,^a Fezza Haider,^a Haritosh Patel,^a Daid A. Khan,^a Zhi Yuan Wang,^b and Yuning Li^{a,*}

DOI: 10.1039/x0xx00000x

www.rsc.org/

We report the photoresponse characteristics of a pyrimido[4,5-*g*]quinazoline-4,9-dione (PQ) based polymer, PPQ2T-BT-24, which served as an active channel layer in organic phototransistors (OPTs). OPTs using this polymer showed very short rise time of 3 ms and fall time of 59 ms, photoresponsivity (*R*) of 0.24 and external quantum efficiency (EQE) of 50 %. When PC₆₁BM was incorporated into PPQ2T-BT-24, a significantly shortened fall time of 8 ms along with a much-improved rise time of 1 ms were realized. These response times are among the best values reported for OPTs. The *R* and EQE of the devices using this polymer blend also increased to 0.88 A W⁻¹ and 189 %, respectively.

Extensive research has been conducted on polymer semiconductors because of their certain desirable properties such as low manufacturing costs, light weight, mechanical flexibility, as well as low-temperature and solution processabilities.^{1,2} These characteristics have led to studies of these materials for potential applications in optoelectronic devices such as organic light-emitting diodes (OLEDs),³⁻⁵ organic photovoltaics (OPVs),⁶⁻⁸ organic thin film transistors (OTFTs),^{2,9,10} and organic phototransistors (OPTs),¹¹⁻¹³ which are a special type of OTFTs. Phototransistors (PTs) that respond in the region from the ultraviolet (UV) to near infrared (NIR) can be used for medical imaging, biological/chemical sensing, communication, environmental monitoring, and security.^{12,14,15} Currently, most commercially available PTs are based on inorganic semiconductor materials such as silicon (Si), silicon carbide (SiC), gallium nitride (GaN), and indium gallium arsenide (InGaAs), which are known to have relatively narrow response spectral windows,^{16,17} limiting their applications. Furthermore, it is difficult to fabricate large area

PTs using inorganic materials due to their complicated fabrication processes.¹⁸ The constrained spectral tunability and poor processability of inorganic semiconductor materials have inspired research into OPTs based on organic semiconductors because the organic semiconductors can be structurally readily tuned to obtain desired band gaps and allow facile device fabrication using solution based processing techniques such as printing.^{12,19,20}

In terms of some device performance parameters, OPTs can be similar or even better than some inorganic PTs. For example, anthra[2,3-*b*]benzo[*d*]thiophene based devices displayed photoresponsivity (*R*) values as high as ~10³ A W⁻¹,²¹ outperforming that of single-crystal silicon phototransistors (~300 A W⁻¹).²² Another important parameter is response time, which determines the operation frequency of a PT device when used as a photoelectrical switch (e.g. a silicon PT can achieve an operation frequency of ~10⁴-10⁵ Hz).²³ Some recently reported OPTs showed relatively short response times of ~10's milliseconds (ms),²⁴⁻²⁶ which are better than those of some inorganic PTs. However, most OPTs²⁷⁻³⁰ show much longer response times (in seconds or longer) than that of a typical silicon PT (~5 μs).²³

Pristine small molecule or polymer semiconductors have been extensively used as the charge transport and photoresponsive channel layers in OPTs. Recently, blending another photoactive component into the organic semiconductor matrix has been used to broaden the spectral coverage and bring about interesting photochemical properties to the OPTs. For example, photochromic small molecules such as spiropyran, diarylethene, and azobenzene have been used as additives in the blends, at the active layer/dielectric interface, and at the active layer/electrode interface to realize reversible photoresponse through photoisomerization of these molecules at different wavelengths.^{31,32} In the more traditional sense the OTFTs operate under gate voltage control, but the OTFTs operation can also be modulated through optical/photochemical control.^{33,34} More recently, blending small molecules and inorganic semiconductors with polymer semiconductors to

^a Department of Chemical Engineering and Waterloo Institute of Nanotechnology (WIN), University of Waterloo, 200 University Ave West, Waterloo, N2L 3G1, Canada.

^b Department of Chemistry, Carleton University, Ottawa, ON, K1S 5B6, Canada.

*Corresponding author: E-mail: yuning.li@uwaterloo.ca; Fax: +1-519-888-4347; Tel: +1-519-888-4567 ext. 31105

[†] Electronic Supplementary Information (ESI) available: experimental section and figures. See DOI: 10.1039/x0xx00000x

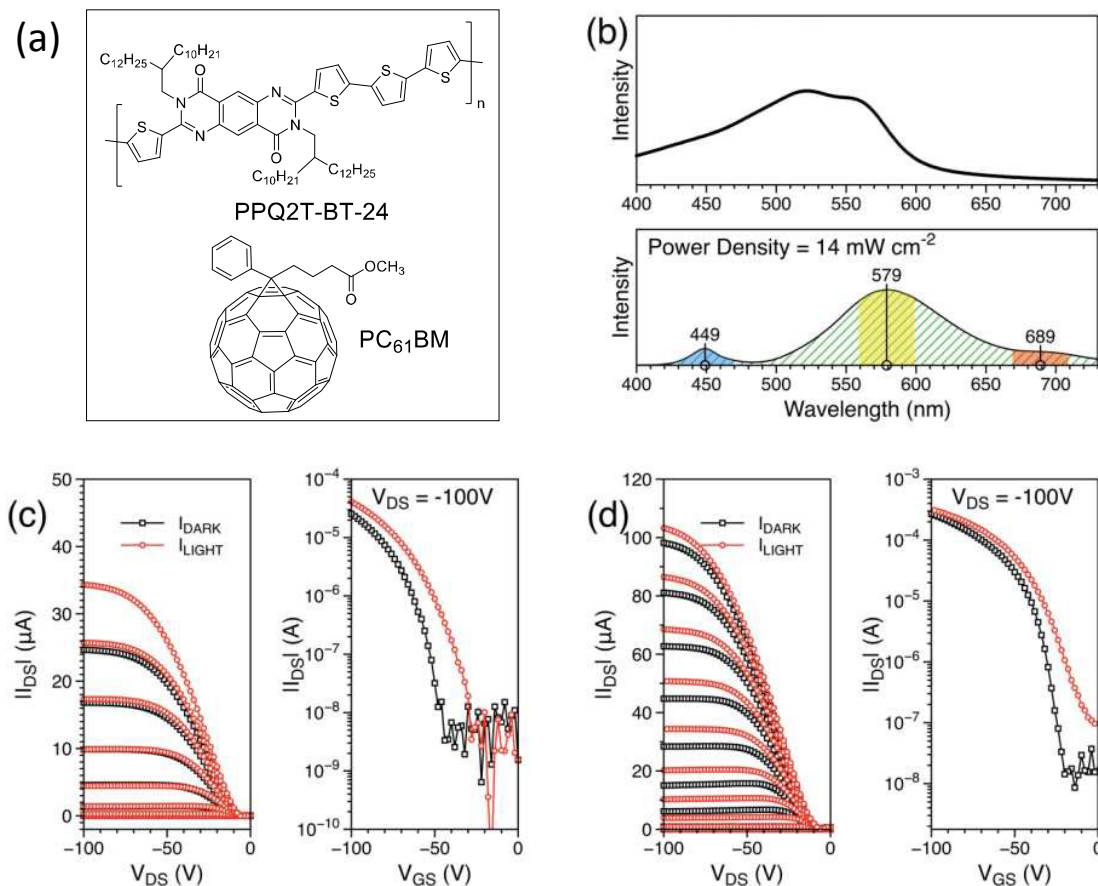


Figure 1. Chemical structure of (a) PPQ2T-BT-24 and PC61BM. (b) The spectral analysis of the light source (bottom) with stacked overlaid UV-Vis-NIR absorption profile of PPQ2T-BT-24 thin film (top). (c) and (d) Output (left) and transfer (right) curves of PPQ2T-BT-24 based (c) and PPQ2T-BT-24:PC61BM based (d) OTFTs measured in the dark and illuminated at 14 mW cm⁻², respectively.

Channel Layer	μ [$\times 10^{-3}$ cm ² V ⁻¹ s ⁻¹] ^a	V_{TH} [V]	I_{ON}/I_{OFF}	Response Time [ms]		R [A W ⁻¹]	P	EQE [%]
PPQ2T-BT-24	3.95 (3.90 \pm 0.06)	-53.1	$\sim 10^5$	Rise time (T_R)	Fall time (T_F)	0.24	1.02×10^2	50
PPQ2T-BT-24:PC61BM	19.22 (16.88 \pm 1.32)	-25.3	$\sim 10^5$	1	8	0.88	0.74×10^2	189

^a average and standard deviation of 5 devices.

Table 1. Summary of OTFT characteristics in dark at 200 °C annealed. Transient photocurrent response times for rise and fall and the utmost photoresponsivity (R) and external quantum efficiency (EQE) achieved.

form active layers with bulk heterojunction structures have also been studied with marked improvements in OPT performance^{18,35-39} compared to their pristine counterparts.

In this study, we report the phototransistor performance of a pyrimido[4,5-g]quinazoline-4,9-dione (PQ) based p-type polymer, PPQ2T-BT-24 (Figure 1a).⁴⁰ OPTs based on this polymer showed very short rise time (T_R) of 3 ms and fall time (T_F) of 59 ms. When an electron acceptor, phenyl-C₆₁-butyric acid methyl ester (PC₆₁BM), was added to PPQ2T-BT-24 (at a 1:1 weight ratio). The T_F of the PPQ2T-BT-24:PC₆₁BM blend was remarkably shortened to 8 ms. At the same time, the T_R was also reduced to a very low value of 1 ms. These response times are among the best values reported so far for OPTs.

To measure the transient photocurrent responses, a 10W LED with a color temperature of 3000 to 3500 K with an

emission peak at 579 nm (Figure 1b bottom) was utilized, which overlaps with the absorption profile of PPQ2T-BT-24 which has a λ_{max} at 562 nm (Figure 1b top).⁴⁰ The typical output and transfer characteristics of the devices based on this polymer in the absence of light (black) and under illumination (red) are shown in Figure 1c). The output curves were swept between 0 V and -100 V for drain voltage (V_{DS}), while gate voltage (V_{GS}) was held constant at values chosen from 0 V to -100 V with 10 V increments. For all devices, there was an increase in drain current (I_{DS}) under illumination compared with their corresponding devices measured in dark. The I_{DS} for the transfer curves, where V_{DS} was held constant at -100 V and V_{GS} was swept from 20 to -100 V, also increased under illumination

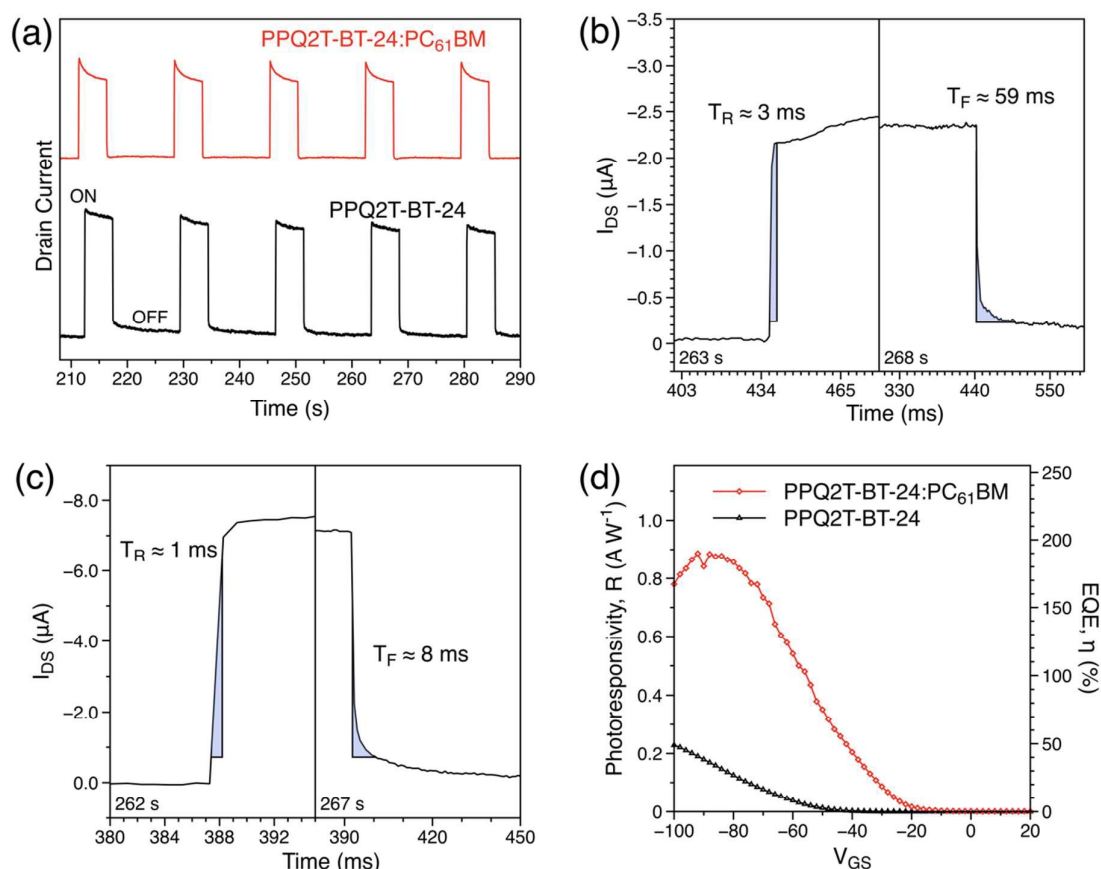


Figure 2. Transient photocurrent responses of (a) PPQ2T-BT-24 and PPQ2T-BT-24:PC₆₁BM as a function of time in response to illumination at 14 mW cm⁻² with 5 s illumination on-state followed by 12 s illumination off-state (dark). (b and c) The estimated rise (T_R) and fall (T_F) time of PPQ2T-BT-24 and PPQ2T-BT-24:PC₆₁BM based devices, respectively. Data collected at 1 ms intervals. (d) The photoresponsivity (R) and external quantum efficiency (EQE, η) of PPQ2T-BT-24 and PPQ2T-BT-24:PC₆₁BM based devices at a constant V_{DS} of -100 V.

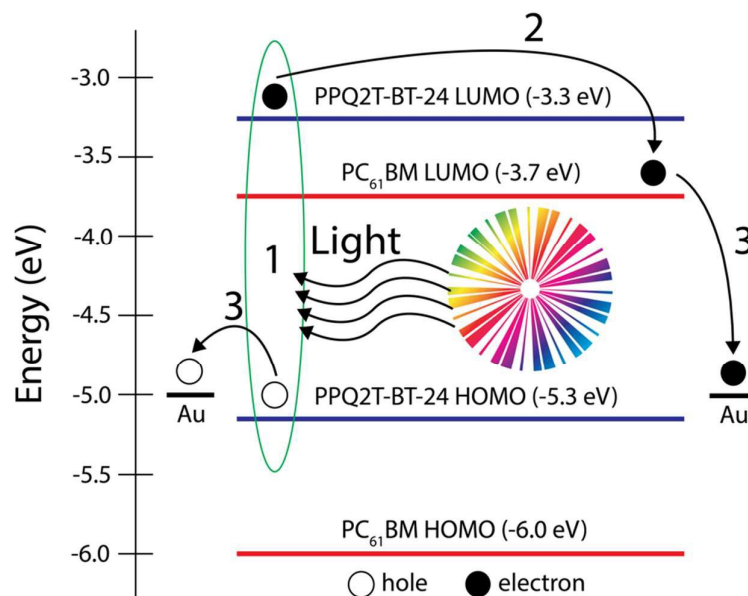


Figure 3. The energy band diagram of the PPQ2T-BT-24:PC₆₁BM based devices showing exciton generation (1), the dissociation of the exciton into electron and hole (2), and the drifting of hole and electron towards the gold (Au) drain and source electrodes, respectively (3). For simplicity, the charges which are generated by the field effect are not illustrated. The HOMO and LUMO energy levels of PC₆₁BM and PPQ2T-BT-24 were taken from ref. 41 and of ref. 40, respectively.

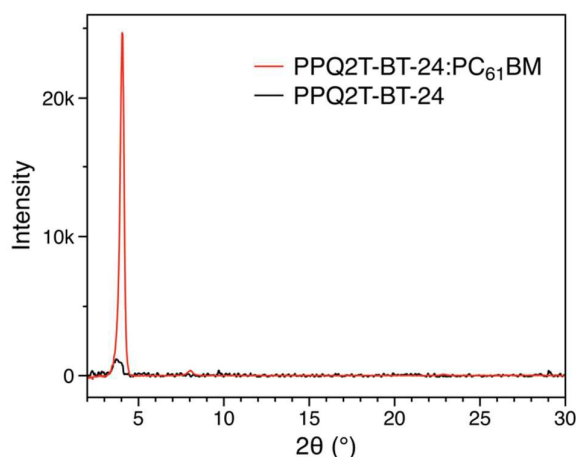


Figure 4. XRD patterns of pristine polymer **PPQ2T-BT-24** and **PPQ2T-BT-24:PC₆₁BM** of 200 °C-annealed thin films.

compared to those in dark. The OTFT devices measured in dark showed typical p-type semiconductor characteristics with hole mobilities in the order of $10^{-3} \text{ cm}^2 \text{ V}^{-1} \text{ s}^{-1}$ (in Table 1), which are comparable with our previously reported values for this polymer.³¹

The transient photocurrent responses of OPTs over time are shown in Figure 2a, where the devices were measured under illumination (on-state) for a 5 s interval, followed by a 12 s interval without illumination (off-state). The response times, T_R and T_F , were measured at constant V_{DS} and V_{GS} values of -100 V. The T_R is defined as the time required for the I_{DS} to increase from 10 % to 90 % of its maximum light on-state value, while the T_F is defined as the time required for the I_{DS} to drop to its 90 % since the light source is turned off.⁴² **PPQ2T-BT-24** demonstrated a T_R of 3 ms and a T_F of 59 ms (Figure 2b). This T_R is shorter than those of many previously reported polymer-based OPTs^{25,26,30,35} and is nearly 4-fold shorter than the reported rise times for some inorganic photodetectors.^{43,44}

The other important parameter for OPTs, photoresponsivity (R), was calculated using the following equation ($R = I_{ill} - I_{dark} / A P_{inc}$)²⁴⁻²⁶ where I_{ill} and I_{dark} are defined as I_{DS} under illumination and in the dark, respectively, A is the channel area, and P_{inc} is the power density of incident light. Figure 2d shows the plot of R as a function of V_{GS} , which ranges from 20 to -100 V, while the V_{DS} was kept constant at -100 V. The R values of the devices are negligible when the V_{GS} was in the range between 20 and -20 V; however, the R values improved greatly as the V_{GS} increased further in the negative direction. At $V_{GS} = -100 \text{ V}$, an R value of 0.24 A W^{-1} was achieved, which is greater than those of some previously reported OPTs.^{26,45} The photocurrent/dark-current ratio ($P = (I_{ill} - I_{dark}) / I_{dark}$) reached 1.02×10^2 at $V_{GS} = -44 \text{ V}$.

An analogous parameter to R is the external quantum efficiency (EQE or η), which is defined as the ratio of generated carriers to incident photons in the transistor channel area. The EQE values can be calculated by using the equation ($EQE = Rhc / \lambda_{peak} e$)⁴⁶ where R is defined previously, h is Planck's constant ($6.62607 \times 10^{-34} \text{ m}^2 \text{ kg s}^{-1}$), c is the speed of light in

vacuum, e is the elementary charge ($1.60218 \times 10^{-19} \text{ C}$), and λ_{peak} is the wavelength of incident light with maximum intensity. For the convenience of EQE calculation, the LED light source was assumed to be monochromatic with a λ_{peak} of 579 nm, similar to the method adopted by Labram *et al.*³⁷ The OPTs with **PPQ2T-BT-24** showed an EQE of up to 50 % (Figure 2d).

Incorporating a fullerene derivative (an n-type semiconductor), such as **PC₆₁BM** (Figure 1a), into a p-type organic semiconductor to form a bulk-heterojunction structure has been reported to be able to improve the OPT performance^{35,42,47} by improving the efficiency of photoinduced charge generation.⁴⁸ Therefore, **PC₆₁BM** was blended with **PPQ2T-BT-24** at a polymer:PC₆₁BM ratio of 1:1 (weight ratio) in order to improve the OPT performance (Figure 1d). In comparison to pristine **PPQ2T-BT-24**, the **PPQ2T-BT-24:PC₆₁BM** blend showed dramatic increases in the I_{DS} together with enhanced mobilities of up to $0.019 \text{ cm}^2 \text{ V}^{-1} \text{ s}^{-1}$ (Figure 1d and Table 1). This mobility enhancement is most likely due to the significantly improved crystallinity of the blend film (to be discussed later). The T_R of the OPTs with this polymer blend decreased to 1 ms (Figure 2a and Figure 2c). The T_F was shortened dramatically to 8 ms, which is an order magnitude lower compared to the pristine polymer. These values are superior to those of some inorganic and hybrid materials based phototransistors^{35,43,44,49-53} and are among the best for small molecule,^{28-30,46,54} polymer,^{25-27,55-60} and polymer blend⁶¹ based phototransistors. Additionally, the EQE values were improved to 189 %. Compared to a photodiode, which has a maximum EQE of 100 %, a phototransistor can realize an EQE greater than 100 % likely due to the photo-multiplication phenomenon enabled by the field-induced tunneling as well as the nature of the semiconductor layer.^{62,63} The maximum EQE value was attained at a lower V_{GS} ($\sim 85 \text{ V}$ shown in Figure 2d) in comparison to that of the pristine polymer (at $V_{GS} = \sim 100 \text{ V}$). This observation may be attributed to the photo-induced shift of V_{TH} due to the photovoltaic effect⁶⁴ and an oversaturation behavior in the I_{DS} .⁶⁵ The photovoltaic effect, where the generated electron-hole pairs (or excitons)

dissociate into electrons and holes (Figure 3), which drift as polarons in opposing directions under a source-drain bias, contributes to the increased I_{DS} and EQE .⁶⁵ In the case of p-type semiconductors, holes flow to the drain contact whereas the electrons accumulate at the source contact where they effectively lower the injection barrier for holes.

The lowered hole injection barrier results in a decrease in contact resistance with a positive shift of V_{TH} (or a reduction in $|V_{TH}|$) thereby increasing I_{DS} .¹² The PC₆₁BM domains in the blend would facilitate the electron transport (*i.e.* movement of electrons towards the source contact) and increase photocurrent³⁵ and thus their accumulation at the source. The lowered hole injection barrier due to the accumulation of electrons at the source might also have contributed to the afore-mentioned photo-multiplication phenomenon. On the contrary, large polaron densities resulting from a change in the power density (*i.e.* increasing power densities of the light source) can increase the chance of recombining polarons, which reduces the I_{DS} and hence the R and EQE values.⁶⁵ If the power density remains constant and large biases are applied, a similar phenomenon may occur.^{42,66-69} At a higher V_{GS} , a larger amount of charge carriers (in this case holes) are injected, producing an excess of holes, which can cross-recombine with the electrons in the polarons. Both of these situations result in minimal contributions to I_{DS} and as a result, "oversaturation" may occur, where the increased portion in I_{DS} caused by the photovoltaic effect slows down and eventually stagnates (saturated), which results in a decrease in EQE and R . For OPTs with the pristine PPQ2T-BT-24, dissociation of photo-generated excitons is less efficient (compared to the blend) where the cross-recombination effect is minimal. Therefore, a monotonic increase in EQE and I_{DS} with V_{GS} is observed for OPT devices based on the pristine PPQ2T-BT-24. With the addition of PC₆₁BM to the polymer, the exciton dissociation is facilitated at the donor (polymer) and acceptor (PC₆₁BM) interface, which is well known for OPV devices.^{16,70,71} Therefore, a greater number of photo-generated holes and electrons exist in the blend channel layer of the OPTs compared with the pristine polymer based devices at high V_{GS} . Consequently, the cross-recombination effect becomes significant and the "oversaturation", occurs, *i.e.*, an optimum V_{GS} was observed. The maximum R of the OPT devices based on the polymer blend increased to 0.88 A W^{-1} . The maximum P value is 0.74×10^2 at $V_{GS} = -20 \text{ V}$. Overall, the OPTs based on the PPQ2T-BT-24 and its blend with PC₆₁BM showed excellent response times and moderate R and P values compared to OPTs with other polymers and polymer blends reported previously (Table S1).

Interestingly, it was noticed that the hole mobility (up to $1.92 \times 10^{-2} \text{ cm}^2 \text{V}^{-1} \text{s}^{-1}$) of the polymer blend increased by an order of magnitude compared to the pristine polymer (up to $3.95 \times 10^{-3} \text{ cm}^2 \text{V}^{-1} \text{s}^{-1}$) when the OTFTs were measured in the dark (Table 1). To investigate the cause for the improved mobility, XRD and AFM were used to probe the molecular ordering and morphologies of the blend and the pristine polymer. The XRD patterns for the polymer blend showed a dramatic increase in crystallinity in comparison to the pristine polymer (Figure 4), which can be attributed to the

antiplasticization effects^{72,73} of PC₆₁BM. AFM height images of the 200 °C-annealed thin film (Figure S1, Supporting Information) indicated that the pristine polymer film was quite smooth with a root-mean-square (RMS) roughness of 0.23 nm. On the other hand, the polymer blend displayed large aggregates with a much larger RMS roughness of 81.0 nm, most likely due to the very high crystallinity of the polymer in the blend as verified by the XRD measurement as well as the aggregation of PC₆₁BM due to the relatively poor solubility of PC₆₁BM and the rapid evaporation of the low boiling point solvent used (chloroform).

The improved mobility of the polymer blend may also account for their improved response times and photoresponsivities. However, the exact effects of mobility on the response times and photoresponsivities are still unclear. In retrospect, although PPQ2T-BT-24 showed relatively low mobility of $\sim 10^{-3} \text{ cm}^2 \text{V}^{-1} \text{s}^{-1}$, it demonstrated very short response times in OPTs compared to the previously reported organic semiconductor materials with much higher mobilities.^{29,30,39,46,54,74,75} Therefore, it seems that the PQ building block might be especially beneficial for achieving short response times. The origin for the short response times observed for this PQ polymer will be the subject of our next step investigation.

Conclusions

In conclusion, the pyrimido[4,5-*g*]quinazoline-4,9-dione (PQ) based polymer, PPQ2T-BT-24, was studied as an active channel layer in organic phototransistors. The devices using the pristine PPQ2T-BT-24 exhibited an R of 0.24 A W^{-1} , a very short T_R of 3 ms, a T_F of 59 ms, and an EQE of 50 %. By blending PC₆₁BM with this polymer, the PPQ2T-BT-24:PC₆₁BM blend (at a 1:1 weight ratio) showed much improved OPT performance with an R of 0.88 A W^{-1} , a T_R of 1 ms, a T_F of 8 ms, and an EQE of 189 %. These results demonstrated that PQ-based polymers are very promising for high performance, particularly fast switching, OPT devices.

Acknowledgements

Financial support of this work by the Natural Sciences and Engineering Research Council (NSERC) of Canada (Discovery Grant # RGPIN-2016-04366) is acknowledged.

Notes and references

1. A. R. Murphy and J. M. Frechet, *Chem. Rev.*, 2007, **107**, 1066-1096.
2. C. Wang, H. Dong, W. Hu, Y. Liu and D. Zhu, *Chem. Rev.*, 2012, **112**, 2208-2267.
3. R. H. Friend, R. W. Gymer, A. B. Holmes, J. H. Burroughes, R. N. Marks, C. Taliani, D. D. C. Bradley, D. A. Dos Santos, J. L. Bredas, M. Logdlund and W. R. Salaneck, *Nature*, 1999, **397**, 121-128.
4. A. P. Kulkarni, C. J. Tonzola, A. Babel and S. A. Jenekhe, *Chem. Mater.*, 2004, **16**, 4556-4573.

5. A. C. Grimsdale, K. L. Chan, R. E. Martin, P. G. Jokisz and A. B. Holmes, *Chem. Rev.*, 2009, **109**, 897-1091.
6. E. Bundgaard and F. C. Krebs, *Sol. Energy Mater. Sol. Cells*, 2007, **91**, 954-985.
7. L. Dou, J. You, Z. Hong, Z. Xu, G. Li, R. A. Street and Y. Yang, *Adv. Mater.*, 2013, **25**, 6642-6671.
8. A. J. Heeger, *Adv. Mater.*, 2014, **26**, 10-27.
9. C. D. Dimitrakopoulos and P. R. L. Malenfant, *Adv. Mater.*, 2002, **14**, 99-117.
10. H. Klauk, *Chem. Soc. Rev.*, 2010, **39**, 2643-2666.
11. H. Dong, H. Zhu, Q. Meng, X. Gong and W. Hu, *Chem. Soc. Rev.*, 2012, **41**, 1754-1808.
12. K. J. Baeg, M. Binda, D. Natali, M. Caironi and Y. Y. Noh, *Adv. Mater.*, 2013, **25**, 4267-4295.
13. P. C. Gu, Y. F. Yao, L. L. Feng, S. J. Niu and H. L. Dong, *Polym. Chem.*, 2015, **6**, 7933-7944.
14. A. Rogalski, J. Antoszewski and L. Faraone, *J. Appl. Phys.*, 2009, **105**, 091101.
15. E. H. Sargent, *Adv. Mater.*, 2005, **17**, 515-522.
16. L. L. Du, X. Luo, F. Y. Zhao, W. L. Lv, J. P. Zhang, Y. Q. Peng, Y. Tang and Y. Wang, *Carbon*, 2016, **96**, 685-694.
17. X. Luo, L. L. Du, W. L. Lv, L. Sun, Y. Li, Y. Q. Peng, F. Y. Zhao, J. P. Zhang, Y. Tang and Y. Wang, *Synth. Met.*, 2015, **210**, 230-235.
18. H. Hwang, H. Kim, S. Nam, D. D. Bradley, C. S. Ha and Y. Kim, *Nanoscale*, 2011, **3**, 2275-2279.
19. Y. Liu, H. F. Wang, H. L. Dong, J. H. Tan, W. P. Hu and X. W. Zhan, *Macromolecules*, 2012, **45**, 1296-1302.
20. Y. S. Kim, S. Y. Bae, K. H. Kim, T. W. Lee, J. A. Hur, M. H. Hoang, M. J. Cho, S. J. Kim, Y. Kim, M. Kim, K. Lee, S. J. Lee and D. H. Choi, *Chem. Commun. (Cambridge, U. K.)*, 2011, **47**, 8907-8909.
21. Y. L. Guo, C. Y. Du, C. A. Di, J. Zheng, X. N. Sun, Y. G. Wen, L. Zhang, W. P. Wu, G. Yu and Y. Q. Liu, *Appl. Phys. Lett.*, 2009, **94**, 143303.
22. N. M. Johnson and A. Chiang, *Appl. Phys. Lett.*, 1984, **45**, 1102-1104.
23. C. Bingruo, G. Fanrong and W. Biao, *Wuhan Univ. J. Nat. Sci.*, 1997, **2**, 431-434.
24. B. Mukherjee, M. Mukherjee, Y. Choi and S. Pyo, *J. Phys. Chem. C*, 2009, **113**, 18870-18873.
25. S. Dutta and K. S. Narayan, *Synth. Met.*, 2004, **146**, 321-324.
26. Q. H. Wang, M. Zhu, D. Wu, G. B. Zhang, X. H. Wang, H. B. Lu, X. H. Wang and L. Z. Qiu, *J. Mater. Chem. C*, 2015, **3**, 10734-10741.
27. H. L. Dong, H. X. Li, E. J. Wang, H. Nakashima, K. Torimitsu and W. P. Hu, *J. Phys. Chem. C*, 2008, **112**, 19690-19693.
28. T. P. I. Saragi, R. Pudzich, T. Fuhrmann and J. Salbeck, *Appl. Phys. Lett.*, 2004, **84**, 2334-2336.
29. K. H. Kim, S. Y. Bae, Y. S. Kim, J. A. Hur, M. H. Hoang, T. W. Lee, M. J. Cho, Y. Kim, M. Kim, J. I. Jin, S. J. Kim, K. Lee, S. J. Lee and D. H. Choi, *Adv. Mater.*, 2011, **23**, 3095-3099.
30. B. Lucas, A. El Amrani, M. Chakaroun, B. Ratier, R. Antony and A. Moliton, *Thin Solid Films*, 2009, **517**, 6280-6282.
31. Y. Wakayama, R. Hayakawa and H. S. Seo, *Sci Technol Adv Mater*, 2014, **15**, 024202.
32. L.-N. Fu, B. Leng, Y.-S. Li and X.-K. Gao, *Chin. Chem. Lett.*, 2016, **27**, 1319-1329.
33. C. Raimondo, N. Crivillers, F. Reinders, F. Sander, M. Mayor and P. Samori, *Proc. Natl. Acad. Sci. U. S. A.*, 2012, **109**, 12375-12380.
34. M. E. Gemayel, K. Borjesson, M. Herder, D. T. Duong, J. A. Hutchison, C. Ruzie, G. Schweicher, A. Salleo, Y. Geerts, S. Hecht, E. Orgiu and P. Samori, *Nat. Commun.*, 2015, **6**, 6330.
35. H. Xu, J. Li, B. H. Leung, C. C. Poon, B. S. Ong, Y. Zhang and N. Zhao, *Nanoscale*, 2013, **5**, 11850-11855.
36. S. Nam, J. Seo, S. Park, S. Lee, J. Jeong, H. Lee, H. Kim and Y. Kim, *ACS Appl. Mater. Interfaces*, 2013, **5**, 1385-1392.
37. H. Han, S. Nam, J. Seo, C. Lee, H. Kim, D. D. Bradley, C. S. Ha and Y. Kim, *Sci. Rep.*, 2015, **5**, 16457.
38. H. Hyemi, N. Sungho, S. Jooyeok, J. Jaehoon, K. Hwajeong, D. D. C. Bradley and K. Youngkyoo, *IEEE J. Sel. Top. Quantum Electron.*, 2016, **22**, 147-153.
39. D. Ljubic, C. S. Smithson, Y. Wu and S. Zhu, *ACS Appl. Mater. Interfaces*, 2016, **8**, 3744-3754.
40. J. Quinn, C. Guo, B. Sun, A. Chan, Y. He, E. Jin and Y. Li, *J. Mater. Chem. C*, 2015, **3**, 11937-11944.
41. M. Yasin, T. Tauqeer, K. S. Karimov, S. E. San, A. Kosemen, Y. Yerli and A. V. Tunc, *Microelectron. Eng.*, 2014, **130**, 13-17.
42. Z. Qi, J. M. Cao, H. Li, L. M. Ding and J. Z. Wang, *Adv. Funct. Mater.*, 2015, **25**, 3138-3146.
43. P. G. Hu, J. Zhang, M. N. Yoon, X. F. Qiao, X. Zhang, W. Feng, P. H. Tan, W. Zheng, J. J. Liu, X. N. Wang, J. C. Idrobo, D. B. Geohegan and K. Xiao, *Nano Res.*, 2014, **7**, 694-703.
44. Z. Wang, M. Safdar, C. Jiang and J. He, *Nano Lett.*, 2012, **12**, 4715-4721.
45. G. B. Zhang, J. H. Guo, J. Zhang, W. T. Li, X. H. Wang, H. B. Lu and L. Z. Qiu, *Dyes Pigm.*, 2016, **126**, 20-28.
46. J. G. Labram, P. H. Wobkenberg, D. D. C. Bradley and T. D. Anthopoulos, *Org. Electron.*, 2010, **11**, 1250-1254.
47. T. D. Anthopoulos, *Appl. Phys. Lett.*, 2007, **91**, 113513.
48. C. H. Lee, G. Yu, D. Moses, K. Pakbaz, C. Zhang, N. S. Sariciftci, A. J. Heeger and F. Wudl, *Phys. Rev. B*, 1993, **48**, 15425-15433.
49. H. Liu, Q. Sun, J. Xing, Z. Zheng, Z. Zhang, Z. Lu and K. Zhao, *ACS Appl. Mater. Interfaces*, 2015, **7**, 6645-6651.
50. F. Yan, J. H. Li and S. M. Mok, *J. Appl. Phys.*, 2009, **106**.
51. X. Fan, X. M. Meng, X. H. Zhang, M. L. Zhang, J. S. Jie, W. J. Zhang, C. S. Lee and S. T. Lee, *J. Phys. Chem. C*, 2009, **113**, 834-838.
52. J. Zhou, Y. Gu, Y. Hu, W. Mai, P. H. Yeh, G. Bao, A. K. Sood, D. L. Polla and Z. L. Wang, *Appl. Phys. Lett.*, 2009, **94**, 191103.
53. Y. Hu, J. Zhou, P. H. Yeh, Z. Li, T. Y. Wei and Z. L. Wang, *Adv. Mater.*, 2010, **22**, 3327-3332.
54. M. Y. Cho, S. J. Kim, Y. D. Han, D. H. Park, K. H. Kim, D. H. Choi and J. Joo, *Adv. Funct. Mater.*, 2008, **18**, 2905-2912.
55. H. J. Nam, J. Cha, S. H. Lee, W. J. Yoo and D. Y. Jung, *Chem. Commun. (Cambridge, U. K.)*, 2014, **50**, 1458-1461.
56. L. R. Fleet, J. Stott, B. Villis, S. Din, M. Serri, G. Aeppli, S. Heutz and A. Nathan, *ACS Appl. Mater. Interfaces*, 2017, **9**, 20686-20695.
57. Y. Lei, N. Li, W.-K. E. Chan, B. S. Ong and F. Zhu, *Org. Electron.*, 2017, **48**, 12-18.
58. M. J. Kim, S. Choi, M. Lee, H. Heo, Y. Lee, J. H. Cho and B. Kim, *ACS Appl. Mater. Interfaces*, 2017, **9**, 19011-19020.
59. X. Liu, Y. Guo, Y. Ma, H. Chen, Z. Mao, H. Wang, G. Yu and Y. Liu, *Adv. Mater.*, 2014, **26**, 3631-3636.
60. M. Kim, H.-J. Ha, H.-J. Yun, I.-K. You, K.-J. Baeg, Y.-H. Kim and B.-K. Ju, *Org. Electron.*, 2014, **15**, 2677-2684.
61. M. Zhu, S. Lv, Q. Wang, G. Zhang, H. Lu and L. Qiu, *Nanoscale*, 2016, **8**, 7738-7748.
62. L. Zhang, T. Wu, Y. Guo, Y. Zhao, X. Sun, Y. Wen, G. Yu and Y. Liu, *Sci. Rep.*, 2013, **3**, 1080.
63. R. M. Pinto, W. Gouveia, A. I. S. Neves and H. Alves, *Appl. Phys. Lett.*, 2015, **107**, 223301.
64. H. S. Kang, C. S. Choi, W. Y. Choi, D. H. Kim and K. S. Seo, *Appl. Phys. Lett.*, 2004, **84**, 3780-3782.

Journal Name

COMMUNICATION

65. K. Wasapinyokul, W. I. Milne and D. P. Chu, *J. Appl. Phys.*, 2009, **105**, 024509.
66. L. C. Ma, Z. R. Yi, S. Wang, Y. Q. Liu and X. W. Zhan, *J. Mater. Chem. C*, 2015, **3**, 1942-1948.
67. W. F. Jin, Z. W. Gao, Y. Zhou, B. Yu, H. Zhang, H. L. Peng, Z. F. Liu and L. Dai, *J. Mater. Chem. C*, 2014, **2**, 1592-1596.
68. Y. Liu, Q. Q. Shi, L. C. Ma, H. L. Dong, J. H. Tan, W. P. Hu and X. W. Zhan, *J. Mater. Chem. C*, 2014, **2**, 9505-9511.
69. M. C. Hamilton, S. Martin and J. Kanicki, *IEEE Trans. Electron Devices*, 2004, **51**, 877-885.
70. R. S. Bhatta and M. Tsige, *ACS Appl. Mater. Interfaces*, 2014, **6**, 15889-15896.
71. C. F. N. Marchiori and M. Koehler, *Synth. Met.*, 2010, **160**, 643-650.
72. B. Sun, W. Hong, H. Aziz, N. M. Abukhdeir and Y. N. Li, *J. Mater. Chem. C*, 2013, **1**, 4423-4426.
73. L. Murphy, B. Sun, W. Hong, H. Aziz and Y. N. Li, *Aust. J. Chem.*, 2015, **68**, 1741-1749.
74. C. S. Smithson, D. Ljubic, Y. Wu and S. Zhu, *J. Mater. Chem. C*, 2015, **3**, 8090-8096.
75. F. Loffredo, A. Bruno, A. D. Del Mauro, I. A. Grimaldi, R. Miscioscia, G. Nenna, G. Pandolfi, M. Petrosino, F. Villani, C. Minarini and A. Facchetti, *Phys. Status Solidi A*, 2014, **211**, 460-466.